

---

# Compton Scatter Compensation Using the Triple-Energy Window Method for Single- and Dual-Isotope SPECT

Takashi Ichihara, Koichi Ogawa, Nobutoku Motomura, Atushi Kubo and Shozo Hashimoto

*Toshiba Nasu Works, Nuclear Medicine Systems Engineering Department, Shimoishigami, Otawara-shi, Tochigi-ken, Japan; Department of Electrical Engineering, College of Engineering, Hosei University, Koganei-shi, Tokyo, Japan; and Keio University School of Medicine, Tokyo, Japan*

---

The spatial distribution of scattered photons varies depending on many factors such as object size and source distribution. We propose a triple-energy window (TEW) scatter compensation method for determining position-dependent Compton scatter. We estimated the count of primary photons at each pixel in the acquired image using the 24% main window centered at the photopeak energy and 3 keV scatter rejection windows on both sides of the main window. We conducted a physical evaluation of this method using phantoms and also applied this method to patients in a clinical trial. The TEW method performed Compton scatter compensation with good accuracy.

J Nucl Med 1993; 34:2216-2221

---

Several factors adversely affect quantitative analysis in gamma camera-based SPECT. Among these, the most significant are Compton-scattered photons mixing into the preset energy window and the attenuation of photons within the human body. Accordingly, several techniques have been proposed for Compton scatter compensation (1-9). In some reports, a Monte Carlo modeling technique is employed to study the distributing properties of scattered photons.

According to these reports, photons generated within the patient are scattered, which affects their direction and energy. These scattered photons then mix into the main energy window. Most of the scattered photons in the main window are single-scatter photons. Furthermore, single-scatter photons vary depending on scatterer distribution and the position of the radioactive source. Consequently, it is necessary to estimate single scatter intensity for each pixel.

We conducted a simulation analysis of scattered photon components mixed into SPECT images by Monte Carlo modeling and proposed a triple-energy window (TEW) compensation method (10) for scattered photons. In prin-

ciple, our method is similar to that proposed by Koral et al. (11). Their method employs the acquisition of spatially dependent energy spectra and estimates scattered photon components for each region on the basis of the energy spectra acquired. Unlike their method, however, our method does not require the acquisition of full energy spectra, but only utilizes total values for three energy windows of the spectra.

We performed a physical evaluation of the TEW method using phantoms and have also applied this method to a patients in a clinical trial.

## MATERIALS AND METHODS

All images in this investigation were acquired with a three-headed, rotating camera dedicated SPECT system GCA-9300A/HG (Toshiba America Medical Systems, Tustin, CA).

### TEW Method for Compton Scatter Compensation

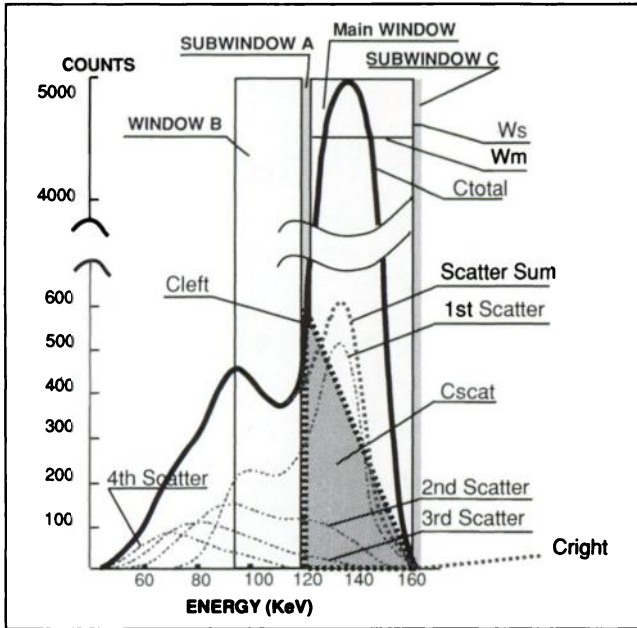
Figure 1 shows the energy spectra of primary and Compton-scattered photons which were simulated for a  $^{99m}\text{Tc}$  line source at the center of a water-filled cylindrical vessel with a 20-cm diameter. The energy spectrum is estimated at the central axis using the Monte Carlo method (14). In the previous paper (10), we located the center of a scatter rejection window at each end of the main window. The scatter rejection windows and the main window thus overlap each other by a width of  $Ws/2$ . In the phantom and clinical studies, it is impossible to acquire using overlapped windows. For clinical implementation of the TEW method to a gamma camera system, we removed the overlap by locating the subwindows adjacent to the main window. We obtained the appropriate location and width of the scatter rejection window based on the analysis of a numerical phantom generated by the Monte Carlo method (15).

Image quality was compared using the root mean square error of SPECT values between the image reconstructed from projections of primary photons and from the corrected projections of scattered photons using the TEW method. Based on these results, the combination of a width of 24% for the main window and a 3 keV scatter rejection window seems appropriate for  $^{99m}\text{Tc}$  (141 keV gamma ray). These widths change depending on the energy of the primary photon.

We obtained the counts from these three windows and estimated the amount of scattered photons mixing into the main window. We employed a trapezoidal approximation for this esti-

---

Received Feb. 10, 1993; revision accepted Aug. 5, 1993.  
For correspondence or reprints contact: Takashi Ichihara, Toshiba Nasu Works, Nuclear Medicine Systems Engineering Dept., 1385 Shimoishigami, Otawara-shi, Tochigi-ken, 324 Japan.



**FIGURE 1.** Position-dependent Compton-scatter compensation method (TEW method) and a simulated energy spectrum of  $^{99m}\text{Tc}$  using Monte Carlo modeling. This figure shows the total energy spectrum (Total), the first to the fourth order scattering (1st Scatter, . . . , 4th Scatter), and the sum of all orders of scattering (Scatter Sum). Most of the scattered photons in the main window are first-order scattered photons. To reduce scattered photons accurately, it is necessary to estimate the scatter sum in the main window, which is shown as a shaded triangle using the counts in narrow scatter rejection windows A and C, adjacent to the main window.

mate. For  $^{99m}\text{Tc}$ , Figure 1 shows the total energy spectrum (Total), the first to the fourth order scattering (1st Scatter, . . . , 4th Scatter), and the sum of all orders of scattering (Scatter Sum). Most of the scattered photons in the main window are first-order scattered photons. To reduce scattered photons accurately, it is necessary to estimate the scatter sum in the main window, which is shown as a shaded triangle using the counts in narrow scatter rejection windows A and C, adjacent to the main window in Figure 1.

The counts and window widths are defined as follows:

- $C_{\text{left}}$  = Counts in scatter rejection window A.
- $C_{\text{right}}$  = Counts in scatter rejection window C.
- $W_s$  = Width of scatter rejection window.
- $W_m$  = Width of main window.
- $C_{\text{total}}$  = Counts in main window.
- $C_{\text{scat}}$  = Counts of scattered photons mixed in main window.
- $C_{\text{prim}}$  = Counts of non-scattered photons in main window.

Then

$$C_{\text{scat}} \cong \left( \frac{C_{\text{left}}}{W_s} + \frac{C_{\text{right}}}{W_s} \right) \frac{W_m}{2}. \quad \text{Eq. 1}$$

Thus, the primary photons for each pixel can be calculated from the following equation:

$$C_{\text{prim}} = C_{\text{total}} - C_{\text{scat}}. \quad \text{Eq. 2}$$

We define the TEW method as Equations 1 and 2. TEW scatter compensation is postprocessing. This method can apply to not only SPECT imaging but planar and dynamic imaging. Data for

TEW scatter compensation can be acquired by any gamma camera system using the three- or two-window acquisition mode.

If each PMT and each camera area has slight offsets, counts in subwindows are unstable and noise increases in estimated scatter images. To avoid these phenomenon, we developed a gamma camera stabilization unit OPTOTUNE™. Uniformity and energy spectrum peak fluctuations were stable using the stabilization unit for the TEW method.

### Phantom Study

**Evaluation of TEW Method Using Hot Rods with a 10-mm Diameter.** To evaluate the proposed scatter-compensation method, we used hot rods 10 mm in diameter in a cylindrical water pool phantom with a 20-cm diameter. Ten hot rods were filled with different activities of  $^{201}\text{Tl}$ ,  $^{99m}\text{Tc}$  or  $^{123}\text{I}$ . In case of single-isotope SPECT, we used six rods to evaluate TEW scatter compensation. The others contained no isotope. To measure the activity of the rods with accuracy, each rod could be taken out of the cylindrical pool phantom. Technetium-99m was to be used for single-isotope studies. In this paper we evaluate the TEW method using  $^{99m}\text{Tc}$  with single-isotope SPECT. For  $^{201}\text{Tl}$  and  $^{123}\text{I}$  myocardial studies, the combination of blood flow ( $^{201}\text{Tl}$ ) and metabolism ( $^{123}\text{I}$ -BMIPP) or the combination of blood flow ( $^{201}\text{Tl}$ ) and the status of sympathetic innervation ( $^{123}\text{I}$ -MIBG) were considered for dual-isotope SPECT. We tested the applicability of TEW method to dual-isotope SPECT using ten rods.

We used Inoue's reconstruction method, including attenuation compensation (12). In the uniform attenuation phantom, the validity of reconstructed SPECT values was assessed. A 10-mm diameter calibration source was used to acquire SPECT data in air and its activity was measured. The SPECT value was measured within a circular ROI with a radius measuring [rod radius + (FWHM of SPECT image)/2]. We then computed the cross-calibration coefficient ( $[\text{mCi}]/[\text{sec}]/[\text{SPECT value}]$ ).

We used the attenuation coefficient of water ( $0.15 \text{ cm}^{-1}$  for the 140 keV gamma ray of  $^{99m}\text{Tc}$ ;  $0.146 \text{ cm}^{-1}$  for the 160 keV gamma ray of  $^{123}\text{I}$ ;  $0.187 \text{ cm}^{-1}$  for the 70 keV x-ray of  $^{201}\text{Tl}$ ).

We defined SPECT values as counts of a reconstructed image pixel. The SPECT value is proportionate to the counts of projection images used for reconstruction. After scatter and attenuation compensation, the SPECT value is proportionate to the true activity of the corresponding position of the radioactive source.

Using  $^{201}\text{Tl}$ ,  $^{123}\text{I}$  and  $^{99m}\text{Tc}$ , cross-calibrated SPECT values versus activity was plotted. Scatter compensation in SPECT can be verified by the graph below. The radioactivity values of the hot rods are plotted on the x-axis. Cross-calibrated SPECT values after accurate attenuation compensation are plotted on the y-axis. In SPECT images, if scatter compensation is perfect, the counts (SPECT value) of a pixel, which has no activity, should be zero. After attenuation compensation, the counts (SPECT value) of pixels with activity are proportionate to the true activity of the corresponding position of the radioactive source. After cross-calibration is performed, the SPECT value should be equal to the true activity of the corresponding position of the radioactive source. If scatter compensation was not done for the SPECT images but was done for the cross-calibration source images, the slope deviated from 1 and the y-intercept was not zero. On the other hand, if scatter compensation was done for the SPECT images and not done for the cross-calibration source images, or if a bad cross-calibration coefficient ( $[\text{mCi}]/[\text{sec}]/[\text{SPECT value}]$ ) was used, the slope deviated from 1 but the y-intercept was zero. In this process, accuracy of the slope value strongly depends on

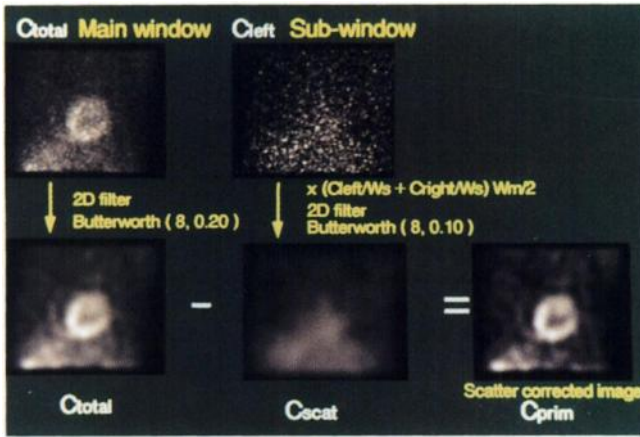


FIGURE 2. Example of scatter compensation for myocardial SPECT images.

determination of the calibration coefficient. Based on this, a y-intercept of roughly zero indicates correct scatter correction.

**Preliminary Clinical Evaluation of <sup>99m</sup>Tc-Tetrafosmin.** Following administration of 370 MBq (10 mCi) of tetrafosmin, images were acquired in continuous rotating mode using a high-resolution, parallel-hole collimator with a 128 × 128 matrix. Images were acquired at 30 sec/projection for a total imaging time of 15 min. Projection data were acquired for two windows. The main window was 24%; the lower scatter rejection window was 3 keV and the upper scatter rejection ( $C_{right}$ ) count was assumed to be zero.

Scatter components were eliminated for each pixel according to Equations 1 and 2. This process was exemplified by the projection data near the LAO 60 position and was shown in Figure 2. The projection data acquired by the main window and scatter rejection windows were subjected to Butterworth filter processing before reconstruction, as shown in Figure 2. The cutoff frequencies of the filter for these two images were 0.2 and 0.1 [cycles/pixel], respectively, with an order of 8. We applied the Butterworth filter to remove high-frequency components. Frequency components higher than the camera resolution were eliminated as noise components. Different cutoff frequency values were applied to main window images and scatter rejection window images. The cutoff frequencies for scatter rejection window images were defined based on the investigation of spatial distribution of multiple-order Compton scatter by Floyd et al. (14,16).

Acquisition was performed under the following conditions:  $C_{right} = 0$ ,  $W_m = 24\%$  and  $W_s = 2.14\%$ . Therefore, Equation 1 can be written as follows:

$$C_{scat} \cong \left( \frac{C_{left}}{2.14} + \frac{0}{2.14} \right) \frac{24}{2}. \quad \text{Eq. 1'}$$

The  $C_{scat}$  images were calculated from Equation 1'. As shown in Equation 2, the scattered photon image was subtracted from the projection image of the main window. The profile curves along line e-f are shown in Figure 3. Image reconstruction was done using filtered backprojection and attenuation correction was not performed.

## RESULTS

### Evaluation of TEW Method

To verify the proposed method of scatter compensation, we performed SPECT acquisition using <sup>201</sup>Tl, <sup>99m</sup>Tc and <sup>123</sup>I and a 10-mm diameter hot rod phantom. After scatter compensation, we used Inoue's method for attenuation compensation. Figure 4 shows the SPECT results obtained for six hot rods of <sup>99m</sup>Tc. The numbers 1–6 correspond to the location of the hot rods. The relative SPECT values were plotted on the y-axis, and the radioactivity values of nuclides sealed in the rod were plotted on the x-axis. The SPECT values after scatter compensation are located very near a straight line which passes roughly through the origin of the graph. Compared to the results obtained without compensation, the degree of improvement is remarkable, and the effect of compensation is evident. For <sup>99m</sup>Tc scatter compensation, we assumed that  $C_{right} = 0$  in Equation 1. Based on these results, it has been shown that, two-window image acquisition is sufficient with <sup>99m</sup>Tc.

In Figures 5 to Figure 7, the cross-calibrated SPECT values were plotted on the y-axis and the radioactivity values of nuclides sealed in the rod were plotted on the x-axis. Figure 5 shows the results of the proposed scatter compensation and attenuation compensation method using five hot rods of <sup>123</sup>I in a water-filled cylindrical phantom. The cross-calibrated SPECT data were fitted to a straight line using the least squares method so that:

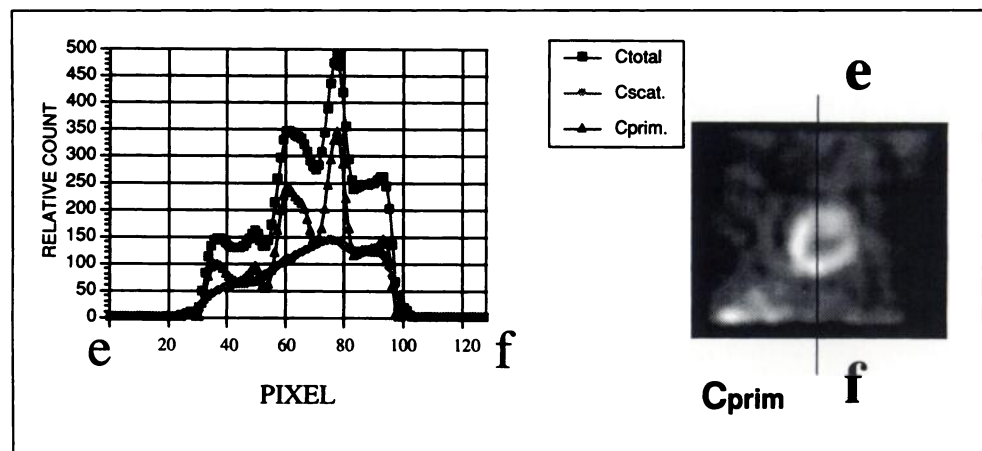


FIGURE 3. Profile curves along line e-f.

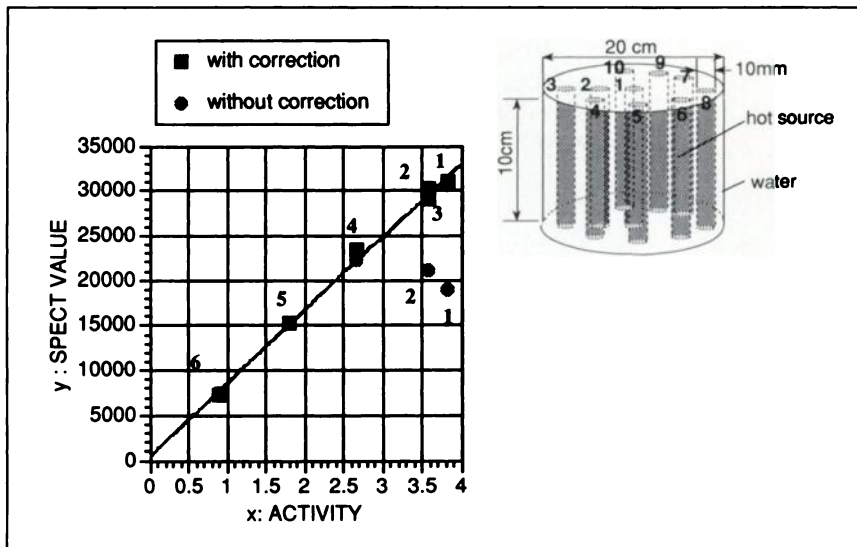


FIGURE 4. Technetium-99m-filled 10-mm hot rod SPECT using an SHR parallel-hole collimator and 10-mm hot rods and pool phantoms.

$$y = 1.087x - 0.009. \quad \text{Eq. 3}$$

Figure 6 shows the same evaluation using hot rods filled with  $^{201}\text{Tl}$  in the same phantom. The cross-calibrated SPECT values were fitted to a straight line:

$$y = 0.912x + 0.011. \quad \text{Eq. 4}$$

Iodine-123 has two photopeaks: 160 keV and 520 keV. Thallium-201 has three main photopeaks: 70 keV, 135 keV and 167 keV. Therefore, it is not possible to suppose that  $C_{\text{right}} = 0$ .

Figure 7 shows the dual-isotope SPECT results obtained for five hot rods of  $^{123}\text{I}$  and five hot rods of  $^{201}\text{Tl}$  using the six-window method. The cross-calibrated SPECT values of scatter compensation using three windows for each isotope were fitted to a straight line:

$$y = 0.908x - 0.0038, \quad \text{Eq. 5}$$

for  $^{201}\text{Tl}$  and,

$$y = 1.01x - 0.0208, \quad \text{Eq. 6}$$

for  $^{123}\text{I}$ .

### Preliminary Clinical Evaluation

**Scatter Compensation for Myocardial Imaging Using  $^{99\text{m}}\text{Tc}$ -Tetrofosmin.** If the image with scatter compensation is subtracted from the image without compensation, it is possible to observe the error caused by scattered photons at the time of SPECT reconstruction. This should not be considered as the distribution of scattered photons, but as errors in the reconstruction calculation. This effect increases from the posterior wall to the liver (spleen), and the level of the effect is not constant as shown in Figure 8. This means that background cancellation with a constant cutoff value is not effective in the display of SPECT images. Accordingly, the calculation error decreases in regions where the posterior wall is in contact with the liver due to scatter compensation. Compared with the data without

compensation, it is evident that the degree of separation is improved. In Figure 8, it can be seen that the SPECT values in the cardiac chambers are almost zero due to scatter compensation. It can safely be said that this is not caused by overcompensation of scattered photons, because absence of overcompensation is verified by profile curve analysis in the data processing of scattered photons as shown in Figures 2 and 3, and Figure 4, which shows the SPECT results obtained for six hot rods of  $^{99\text{m}}\text{Tc}$ . If we know the ratio between the concentration of  $^{99\text{m}}\text{Tc}$ -tetrofosmin in the blood after intravenous injection and myocardial uptake, we can prove that the SPECT values in the left ventricle become zero.

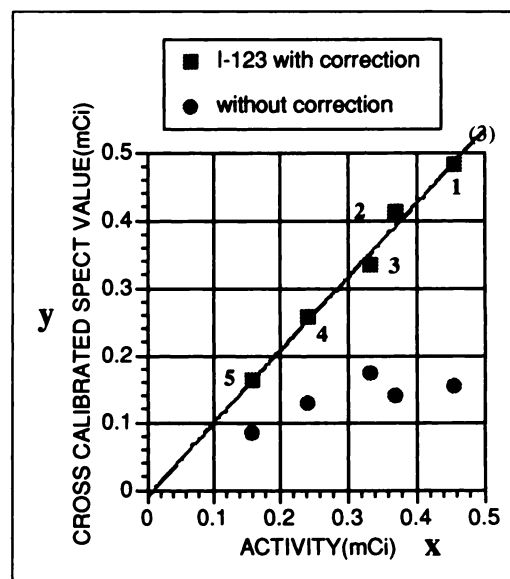


FIGURE 5. Iodine-123-filled 10-mm hot rod SPECT using an SHR parallel-hole collimator.

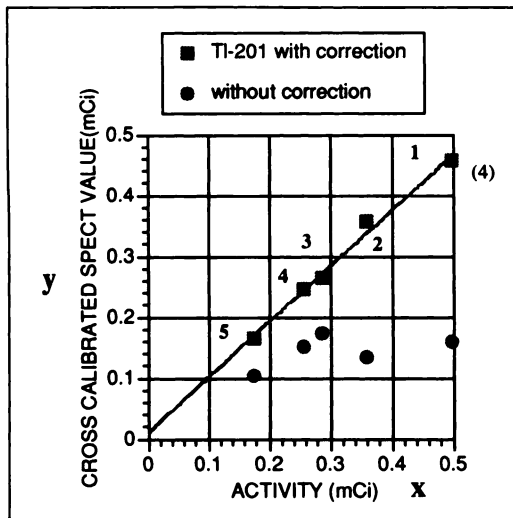


FIGURE 6. Thallium-201-filled 10-mm hot rod SPECT using an SHR parallel-hole collimator.

### DISCUSSION

An experiment was carried out on a hot rod phantom to evaluate the compensation of scattered photons. When the shape of the phantom is known and distribution of attenuation coefficients is uniform. For such an ideal situation, Inoue's method of SPECT reconstruction is capable of giving a complete analytical solution, including attenuation compensation. For this reason, his method was used for this evaluation. After scatter compensation, attenuation compensation was performed ideally. A graph was drawn by plotting the cross-calibrated SPECT values against the radioactivity of the rods. The cross-calibrated SPECT val-

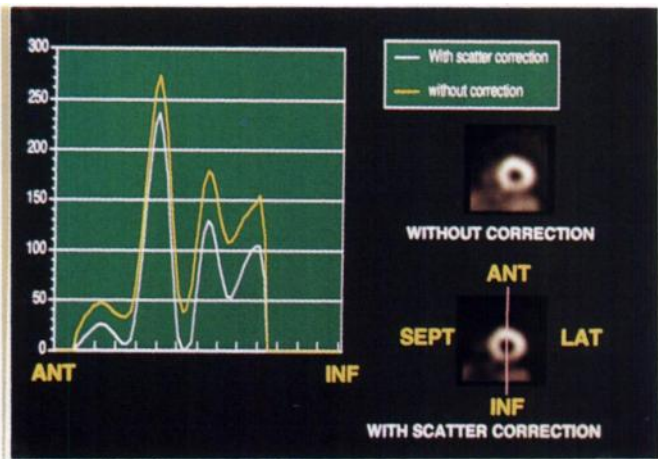


FIGURE 8. Result of scatter compensation for myocardial SPECT images.

ues were fitted to a straight line. In the case of the single-isotope SPECT study, straight lines 3 and 4 are slightly offset from the origin. The accuracy of the y-intercept values was within 2% of the maximum activity of the hot rods. If attenuation and scatter compensation were performed ideally, the gradient of these straight lines would be unity. The gradients of straight lines 3 and 4 were 1.087 and 0.912, respectively. At this time, net accuracy for measurements of activity using SPECT, including cross-calibration, was estimated within  $\pm 10\%$ . These values strongly depend on the cross-calibration process.

For dual-isotope SPECT of  $^{201}\text{Tl}$  and  $^{123}\text{I}$  using six windows, y-intercept values decreased 0.01 mCi. In spite of the cross-talk effect from  $^{201}\text{Tl}$  photons of 135 keV and 167

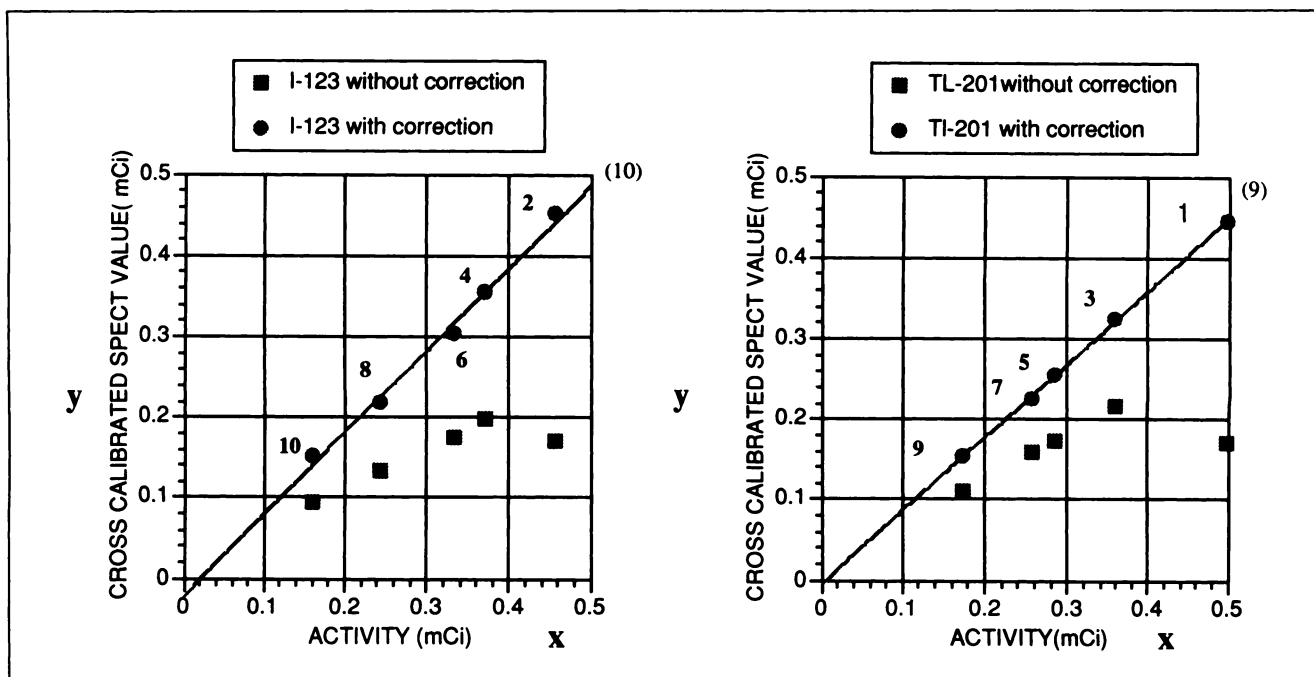


FIGURE 7. Dual-isotope SPECT results for five rods of  $^{123}\text{I}$  and  $^{201}\text{Tl}$ .

keV to the  $^{123}\text{I}$  160 keV main window, the gradients of straight lines 5 and 6 were almost the same, as in the single-isotope SPECT study. When using a nuclide with multiple energy peaks such as  $^{123}\text{I}$ , the results for the rod phantom showed that three windows were required. But in the case of a nuclide with a single-energy peak of emitted photons such as  $^{99\text{m}}\text{Tc}$ , the scattered photons can be eliminated by using two windows: a main window and a scatter-rejection window to the left of the main window.

For a preliminary clinical evaluation, the proposed scatter compensation method required a 24% main window image and one or two 3-keV scatter rejection window images which were acquired with one scan using a three- or two-window acquisition. Scatter compensation was performed at postprocessing. Projection data from a 24% main window and one or two 3-keV scatter rejection windows can be reconstructed either as conventional SPECT images without scatter compensation or as SPECT images with scatter compensation. These data are easily compared. Clinical evaluation for the proposed scatter compensation method can be done without affecting routine SPECT studies. This is one of the advantages of the TEW method. In myocardial imaging using  $^{99\text{m}}\text{Tc}$ -tetrofosmin, the fact that SPECT values in the cardiac chambers become almost zero is an expected result following the report concerning the dynamics after the administration of  $^{99\text{m}}\text{Tc}$ -tetrofosmin (13). Within 30 min to 1 hr after intravenous administration, the myocardial uptake is 1.8% (injected dose) and blood concentration is 0.2% (injected dose/liter). If the fluctuation in cardiac chamber volume is considered, this result appears reasonable. In this way, SPECT values become zero in regions where there is no distribution of radiopharmaceuticals. This fact contributes significantly to reproducibility and quantitative accuracy in the identification of regions of distribution and regions of ischemia on the data display when clinical images are evaluated.

## CONCLUSIONS

We have determined that the TEW method using one main energy window and two scatter rejection windows

accurately compensates for Compton-scatter. The TEW method is easier to perform, contributing significantly to quantitative analysis in single- or dual-isotope studies. In the future, it will be possible to apply this method to clinical use for routine examinations.

## REFERENCES

1. Bloch P, Sanders T. Reduction of effects of scattered photons on a sodium iodine imaging system. *J Nucl Med* 1972;25:67-72.
2. Floyd CE, Jaszczak RJ, Harris CC, Coleman RE. Energy and spatial distribution of multiple order Compton scatter in SPECT: a Monte Carlo investigation. *Phys Med Biol* 1984;29:1217-1230.
3. Bachrach SL, Green MV, Bonow RO, Findly SL, Daube-Witherspoon ME, Larson SM. The effect of energy window on cardiac ejection fraction. *J Nucl Med* 1988;29:385-391.
4. Jaszczak RJ, Greer KL, Floyd CE Jr, Harris C, Coleman E. Improved SPECT quantification using compensation for scattered photons. *J Nucl Med* 1984;25:893-900.
5. Jaszczak RJ, Floyd CE Jr., Coleman E. Scatter compensation techniques for SPECT. *IEEE Trans Nucl Sci* 1985;32:786-793.
6. Axelsson B, Masaki P, Israelsson A. Subtraction of Compton-scattered photons in single photon emission computerized tomography. *J Nucl Med* 1984;25:490-494.
7. Hamill JJ, De Vito RP. Scatter reduction with energy-weighted acquisition. *IEEE Trans Nucl Sci* 1989;36:1334-1339.
8. De Vito RP, Hamill JJ. Determination of weighting functions for energy-weighted acquisition. *J Nucl Med* 1991;32:343-349.
9. King MA, Hademenos GJ, Glick SJ. A dual-photopeak window method for scatter compensation. *J Nucl Med* 1992;33:605-612.
10. Ogawa K, Harata Y, Ichihara T, Kubo A, Hashimoto S. A practical method for position-dependent Compton scatter compensation in single photon emission CT. *IEEE TMI* 1991;10:408-412.
11. Koral KF, Wang X, Rogers WL, Clonthorene NH, Wang X. SPECT Compton-scatter compensation by analysis of energy spectra. *J Nucl Med* 1988;29:195-202.
12. Inoue T, Kose K, Hasegawa A. Image reconstruction algorithm for single-photon emission computed tomography with uniform attenuation. *Phys Med Biol* 1989;34:299-304.
13. Kubo A, Nakamura K, Hashimoto J. Phase I clinical trial of a new myocardial imaging agent  $^{99\text{m}}\text{Tc}$ -PPN 1011. *Jpn J Nucl Med* 1992;29:1165-1176.
14. Ogawa K, Harata Y, Ichihara T, Kubo A, Hashimoto S. Estimation of scatter component in SPECT planar image using a Monte Carlo method. *Jpn J Nucl Med* 1990;27:467-475.
15. Ogawa K, Chugo A, Ichihara T, Kubo A, Hashimoto S. Quantitative image reconstruction using position-dependent scatter correction in single photon emission ct. *Conf Rec 1992 IEEE Nuc Sci Sym* 1992;2:1011-1013.
16. Floyd CE, Jaszczak RJ, Harris CC, Coleman RE. Energy and spatial distribution of multiple-order Compton scatter in SPECT: a Monte Carlo investigation. *Phys Med Biol* 1984;29:1217-1230.